JOURNAL OF MATERIALS SCIENCE **34** (1999) 2781–2787

The relationship between the dynamic mechanical relaxations and the tensile deformation behaviour of polyethylene

R. G. MATTHEWS, I. M. WARD*
IRC in Polymer Science and Technology, The University of Leeds, Leeds LS2 9JT, UK

G. CAPACCIO
BP Chemicals Ltd., P.O. Box 9, Bo'ness Road, Grangemouth, Stirlingshire, FK3 9XH, UK
E-mail: i.m.ward@leeds.ac.uk

The mechanical relaxation behaviour of high and linear low density polyethylenes has been examined using tensile dynamic mechanical measurements and compared to the deformation behaviour observed in tensile drawing. In this way the relationship between the mechanical relaxations and the tensile deformation has been investigated. It is shown that the brittle-ductile transition relates to the γ-relaxation while the yield behaviour is related to the interlamellar shear process and the c-shear process.

1. Introduction

The mechanical relaxations in polymers correspond to the particular mechanisms of thermally activated molecular motion and therefore to the general mobility of the polymer chains, an important factor in determining the type of deformation. If there is little chain mobility the polymer will fail in a brittle manner. If the chains are free to move, however, the material will yield or, at higher temperatures, deformation will be homogeneous and it will behave as a viscoelastic-plastic solid. Therefore, if the mechanical relaxations of polyethylene are compared to the deformation behaviour in a tensile test there should be an observable relationship.

There is a large body of literature about the relaxation processes that occur in polyethylene [1–5] showing that high density polyethylene (HDPE) has two major relaxations while low density polyethylene (LDPE) shows three. Both HDPE and LDPE exhibit a γ-relaxation, occurring between -150 and $-110\,^{\circ}$C, which is due to the onset of short range conformational changes in the amorphous regions.

The β-relaxation is thought to relate to the amorphous regions because its magnitude increases with decreasing crystalline fraction [1] and the mechanism is envisaged as shearing of the amorphous material between the lamellae which is activated by the relaxation of branch points. In LDPE the α-relaxation is a crystalline relaxation attributed to c-shear of the chains within the lamellae activated by the rearrangement of the fold surface [4, 5]. In HDPE the α-relaxation appears to be a composite relaxation relating to the crystalline region. At least two possible relaxation processes have been proposed, one by Takayanagi [6] relating to the motion of chains within the crystalline region, and a relaxation due to interlamellar shearing, similar to the β-relaxation in LDPE, but activated by c-shear. The latter proposal is elaborated in a separate paper [7], and takes into account previous research in the area, especially by Boyd and Stachurski and Ward [2–5].

There has also been significant investigation of the drawing behaviour of polyethylene [8–13]. It is known that at low temperatures polyethylene fails in a brittle manner whereas at higher temperatures it fails through strain softening with the formation of a neck. As the temperature is raised further, polyethylene undergoes cold drawing where the sample does not fail on the formation of the neck but the neck propagates along the length of the sample.

The work of Brooks *et al.* [11–13] looked at the yielding behaviour of polyethylene, in particular the "double yield point" phenomenon, and showed that there is a relationship between the mechanical relaxations and the yielding behaviour. The first yield point, found using a variation of the Considère construction, corresponds to the end of the initial recoverable deformation produced by lamellar reorientation. The second yield point, seen as the load drop at higher applied strains, is associated with the formation of a sharp neck due to the irreversible destruction of lamellae by c-shear.

In this paper the connection between the mechanical relaxations and the deformation is further investigated in both high and linear low density polyethylenes.

2. Experimental

2.1. Materials

The characteristics of the polymers used are shown in Table I. Two linear low density grades (LL-BU and

* Author to whom all correspondence should be addressed.

TABLE I Chemical characterisation of high and linear low density polyethylenes

Sample	Branch type	Branch content/ 10^3 C atoms	$\bar{M}_w$	$\bar{M}_n$
HDPE		<0.1	131,000	19,000
LL-BU	Ethyl	21.0	126,000	30,000
LL-OCT	Hexyl	21.0	130,000	30,000

LL-OCT) were examined because they have different side groups and different distributions of the side groups along the length of the polymer chains and it is of interest to see how this affects their properties.

The polymers were provided in granule form and so compression moulding in a hot press, at 160 °C and a pressure of 3 MPa, was used to produce 0.5 mm thick sheet. Following much previous research in this laboratory, samples with different morphologies were produced by two standard cooling regimes: quenching (Q) or slow cooling (SC). Quenched samples were produced by removing the sheets from the press after 5 minutes and rapidly cooling them to room temperature in a water bath. Slow cooled samples were produced by cooling the plates under pressure in the hot press at a rate of 2 K min^{-1}.

2.2. Dynamic mechanical measurements

The dynamical mechanical measurements described in this paper were performed on a rig designed and built in-house as described in previous publications [14]. The tests were performed on samples of the same length, 4.5 cm, and width, 2 mm, so that the aspect ratio was always greater than 20 to minimise end effects. The storage modulus and loss factor measurements were made using a sinusoidal tensile strain of 0.05%, with an average strain of 0.1%, so that the sample was always under tension. Measurements were undertaken at a range of frequencies between 0.1 and 30 Hz.

The test temperature was controlled to an accuracy of ±0.5 °C by blowing N_2 gas over the sample. The heating regime can have a major influence on the dynamic mechanical results [1] because rapid heating can move the sample out of thermodynamic equilibrium. To avoid this the sample temperature was changed at a rate of 2 K min^{-1} which the work of Gibson *et al.* [14] has shown keeps the sample in thermodynamic equilibrium.

2.3. Tensile drawing experiments

The mechanical behaviour was examined by drawing samples on an Instron tensile testing machine in the temperature range from –130 °C to room temperature. Drawing was performed in an Instron mounted cryostat which was cooled using nitrogen gas. An initial strain rate of 2×10^{-3} s^{-1} was used. Samples, with a gauge length of 1.8 cm and 5 mm wide, were cut from moulded sheets using a dumbbell cutter. Drawing continued past the yield point until failure or a significant length of neck had been formed.

2.4. Measurement of crystalline fraction and lamellar thickness

A Perkin Elmer DSC3 Differential Scanning Calorimeter was used to record the melting behaviour at a heating rate of 10 K min^{-1}, from which the crystallinity and the lamellar thickness were obtained. The crystallinity was determined as

$$a_c = \frac{\Delta H_{samp}}{\Delta H^0}$$

where ΔH_{samp} is the enthalpy of melting per gram for the sample and ΔH^0 (310 Jg^{-1}) [15] is the enthalpy of melting per gram of an infinite crystal. ΔH_{samp} is calculated from the area of the melting peak. The level of accuracy obtained for the crystalline fraction measurements on the branched materials is not particularly high because of the wide melting endotherms.

The lamellar thickness, L, was found from the melting temperature, T_p, using the Hoffman-Weeks equation [16]:

$$L = \frac{T^0 2\sigma}{H_m(T^0 - T_p)}$$

where σ is the surface free energy of the basal face (80×10^{-3} Jm^{-2}), H_m is the enthalpy of melting per unit volume (310 J cm^{-3}) and T^0 is the equilibrium temperature of an infinite crystal (418.7 K) [15]. Errors in the lamellar size arise from uncertainties in the values of the different parameters, especially T^0, but these do not affect relative behaviour, while errors in T_p arising from superheating effects are considered negligible.

3. Results and discussion

3.1. Characterisation of the structure of the isotropic samples

The crystalline mass fractions and lamellar thicknesses of quenched and slow cooled samples are shown in Table II. It should be noted that these calculations relate to the maximum lamellar thickness and that the endotherms show a wide melting range indicating the presence of much thinner lamellae. Calculations of the lamellar size using measurements of long period and crystallinity give considerably lower values for the lamellar thickness. Nevertheless, it can be seen that the lamellar thickness is dependent on the cooling regime for all three polyethylene grades with slow cooling producing higher lamellar thicknesses than quenching for the same grade. A significantly higher crystalline fraction is also found in slow cooled HDPE but for LL-BU

TABLE II Morphology of Isotropic Polyethylenes examined by DSC

Sample	Crystal fraction (a_c%)	Lamellar thickness (nm)
LL-BU(Q)	37	9.2
LL-BU(SC)	40	10
LL-OCT(Q)	39	8.1
LL-OCT(SC)	42	8.8
HDPE(Q)	62	12.3
HDPE(SC)	72	14.8

and LL-OCT the difference observed is only just above experimental error, which is high for these materials because of the very wide range of the melting endotherm.

The methylene sequence length between branch points is seen to be a major factor in determining the lamellar thickness because the side groups are not easily included in the lamellae. This is illustrated by HDPE possessing a much higher lamellar thickness than LL-BU which itself is slightly greater than for LL-OCT. The linear low density materials also have much lower crystalline fractions because of the greater number of side groups.

3.2. Mechanical relaxations and drawing behaviour of HDPE

In Fig. 1 relaxation curves are shown for both quenched and slow cooled samples of HDPE and it can be seen that there are some differences. In the slow cooled sample the peak in the γ-relaxation occurs at a slightly higher temperature than in the quenched sample. Table II shows that the slow cooled sample has the higher lamellar thickness and crystalline fraction. The γ-relaxation is considered to occur predominantly in the amorphous region [1] but the differences observed between the quenched and slow cooled samples suggest that there may also be a significant crystalline contribution, as concluded by some previous workers.

The relaxation processes associated with the γ-relaxation are crankshaft mechanisms [3] which are activated at slightly different temperatures in the amorphous and crystalline regions due to their different levels of free volume. The motions would occur first in the amorphous region because it has a higher level of free volume and so the decrease in the low temperature side of the peak corresponds to the higher crystalline fraction in the slow cooled material. The free volume in the crystalline regions probably relates to defects in the lamellae.

The α-relaxations in the quenched and slow cooled samples also show some differences with the onset occurring approximately 10 °C lower for the quenched samples. The α-relaxation in the high density material is activated by c-shear within the lamellae and Hoffman *et al.* [17] showed that the greater degree of co-operative motion required for c-shear to occur through thicker lamellae does raise the temperature of the α-relaxation.

The drawing behaviour was investigated for both the quenched and slow cooled samples of HDPE and brittle failure was only observed in the slow cooled samples tested below –130 °C. This suggests that the brittle-ductile transition is related to the small scale molecular motions associated with the γ-relaxation. It was also observed that the quenched samples cold drew across the whole temperature range, while the slow cooled ones failed by necking rupture up to temperatures around –100 °C. Even in these samples, however, significant lengths were drawn into the neck before failure.

The yield stresses and strains for quenched samples are shown in Fig. 2a and b, respectively. The yield stress seems to have an almost linear dependence on the temperature and no apparent relationship with the relaxation spectrum. The yield strain, on the other hand, is independent of temperature at temperatures below –20 °C but above this, with the onset of the α-relaxation, it increases linearly. Similar results were obtained for the slow cooled samples but were less clear than for the quenched material, perhaps due to greater sensitivity to sample flaws in the slow cooled material.

The true stress-strain curves obtained from the drawing of both quenched and slow cooled samples were also examined and apart from the brittle failure of the

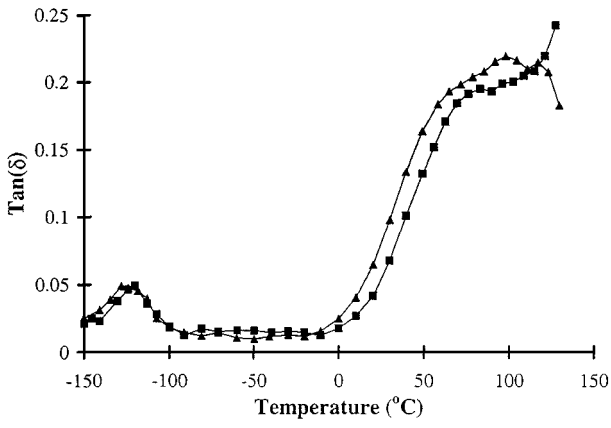

Figure 1 The mechanical relaxations in quenched, ▲, and slow cooled, ■, samples of HDPE.

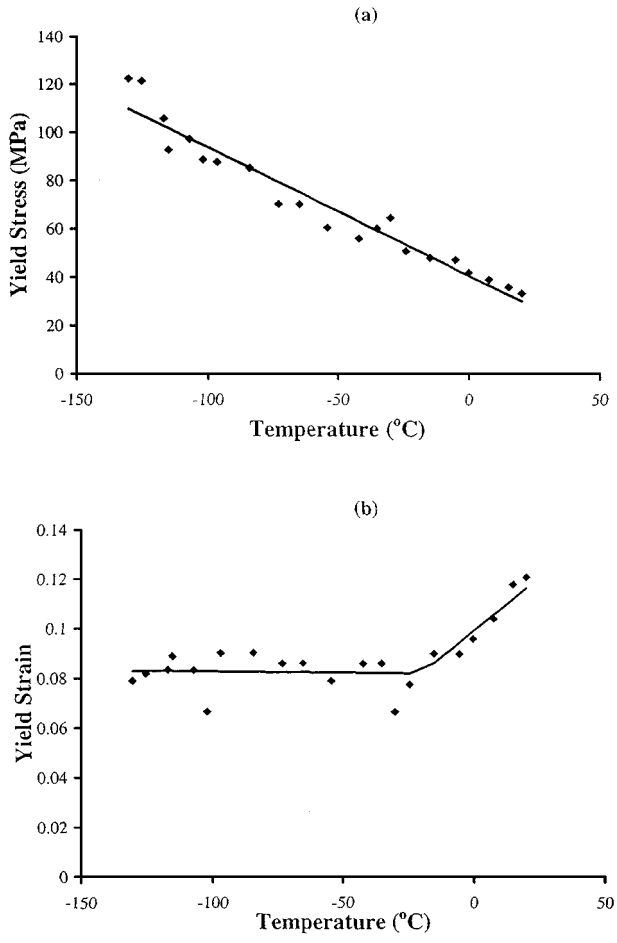

Figure 2 The yield behaviour of quenched HDPE drawn at an initial strain rate of 2×10^{-3} s^{-1} (a) yield stress and (b) yield strain.

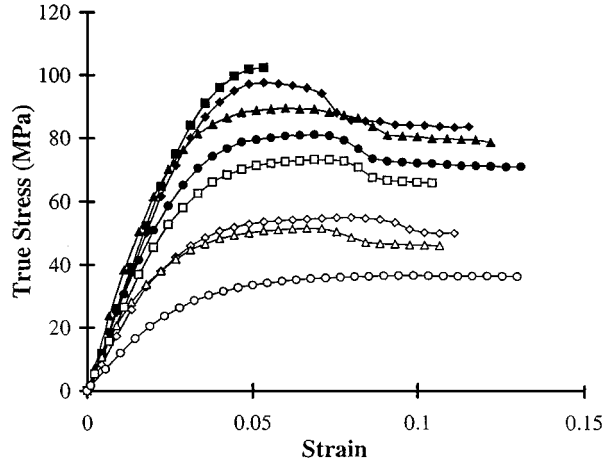

Figure 3 True stress-strain curves obtained from the uniaxial drawing of slow cooled HDPE at an initial strain rate of 2×10^{-3} s^{-1}. Temperature, ■, −133 °C; ♦, −126 °C; ▲, −113 °C; ●, −96 °C; □, −57 °C; ◇, −40 °C; △, −24 °C; and ◯, 20 °C.

slow cooled material, at the lowest temperatures, the same behaviour was observed in both materials so only the slow cooled results are given in Fig. 3. The curve obtained from the drawing of slow cooled HDPE at −133 °C is given because it is the only example of fracture seen for any of the materials. This curve shows that this sample does not extend perfectly elastically even at this low temperature. This, however, is to be expected because the loss peak shows that molecular motions do occur at this temperature. The other curves obtained below 0 °C, i.e., before the onset of the α-relaxation, show that there is a clear load drop as the neck is formed and cold drawing begins. At temperatures above 0 °C no load drop is seen so the interlamellar shearing within the samples, the α-relaxation mechanism, clearly affects the stress-strain behaviour.

The drawing behaviour observed for the quenched HDPE is in agreement with the results of Brooks *et al*. [11, 12]. They concluded that the observed transition in

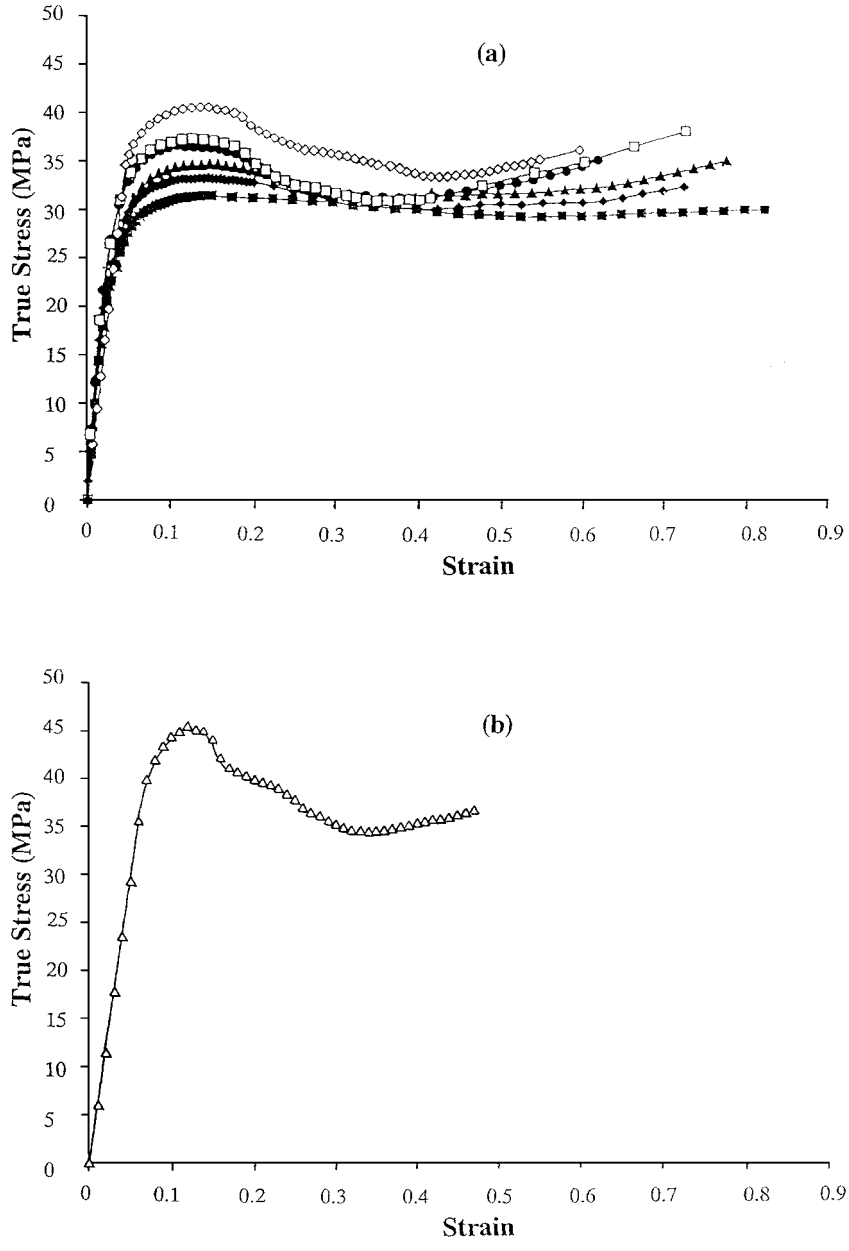

Figure 4 True stress-strain curves obtained from the uniaxial drawing of slow cooled HDPE at room temperature at (a) strain rates, ■, 0.002; ♦,0.004; ▲,0.008; ●,0.016; □ 0.02; ◇,0.04; and (b) △, 0.08 s^{-1}.

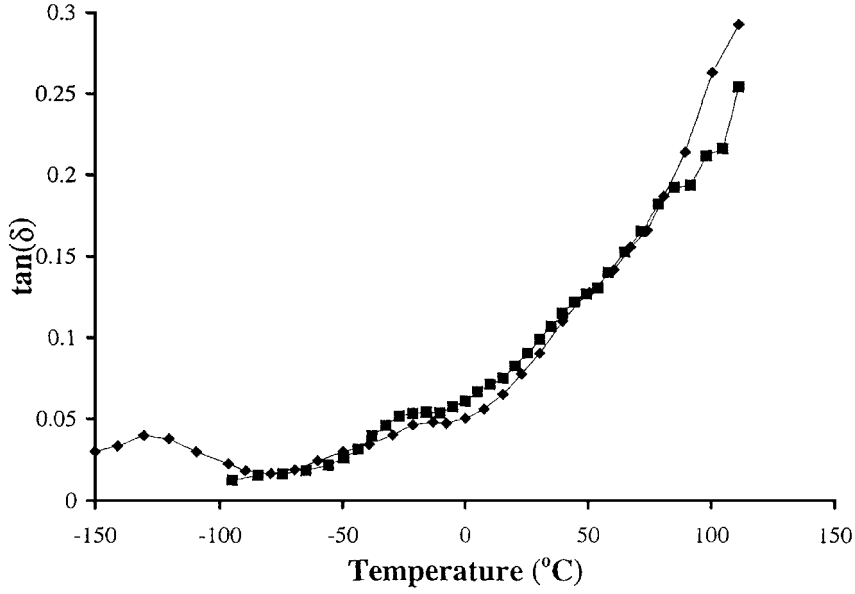

Figure 5 The mechanical relaxations in slow cooled samples of LL-BU, ♦, and LL-OCT, ■.

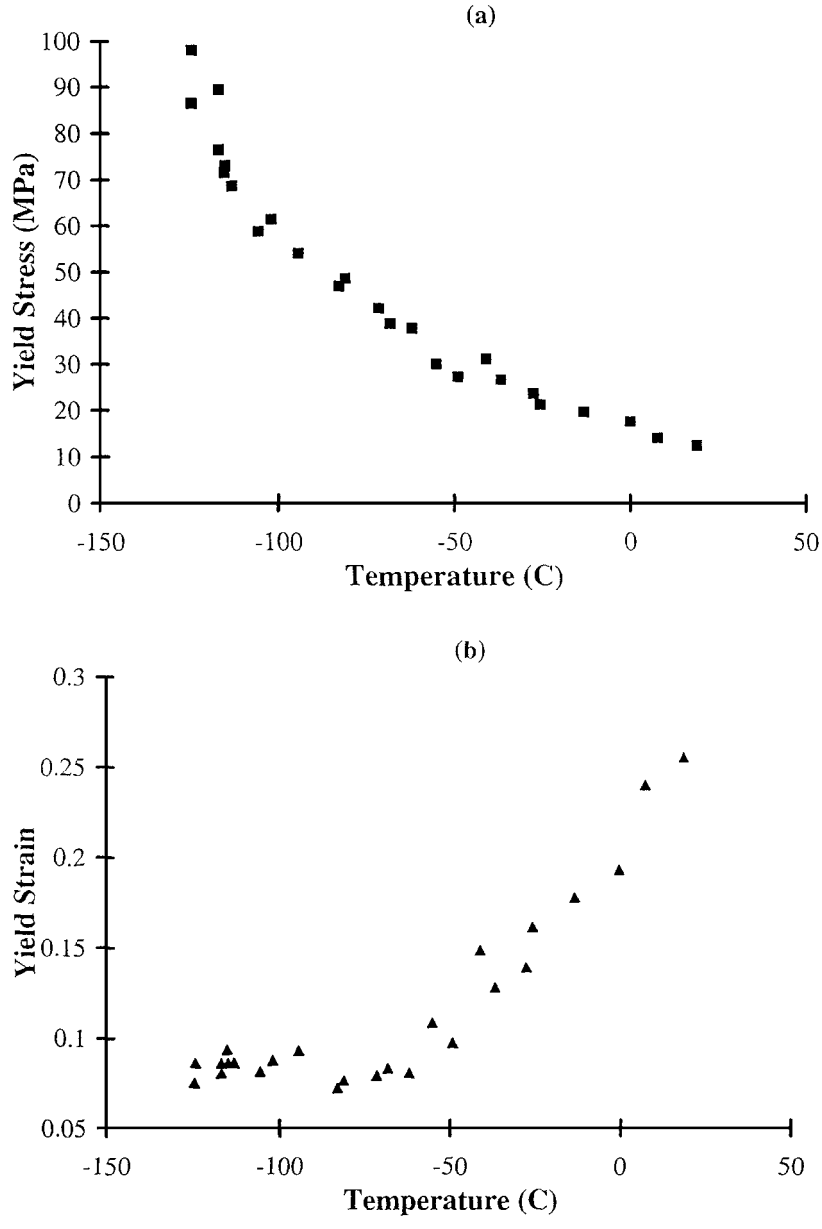

Figure 6 The yield behaviour of slow cooled LL-BU drawn at an initial strain rate of $2 \times 10^{-3}\ s^{-1}$ (a) yield stress and (b) yield strain.

the drawing behaviour at −20 °C, Fig. 2b, is due to the lamellar reorientation process associated with the first yield point being "frozen-out" or being localised to the neck. The localisation is indicated by the increase in the degree of strain softening at the yield point as the temperature decreases, as seen in Fig. 3. This transition is related to the α-relaxation because it is with the onset of the interlamellar shear process that reorientation of the lamellae can occur.

To separate the different yielding mechanisms, samples were drawn uniaxially at room temperature at a number of different strain rates and the resulting true stress-strain curves is shown in Fig. 4a and b. It can be seen that at the lowest strain rates only one yield point is observable (Fig. 4a) but at the highest strain rates the two different yield mechanisms have been successfully separated by increasing the strain rate (Fig. 4b). The mechanisms are separable because they have different activation energies with the interlamellar shear process, which is related to the first yield point, having a higher activation energy than the c-shear mechanism, which is related to the second yield point [7]. The lower activation energy of the c-shear mechanism means that the second yield point is shifted up to higher strains with increasing strain rates.

3.3. Mechanical relaxations and drawing behaviour of LL-BU and LL-OCT

The relaxation curves of the LLDPE's are shown in Fig. 5. Only slow cooled morphologies were examined. LL-BU shows the α, β and γ relaxations as would be expected. In LL-OCT, where a more limited temperature range was measured the α and β relaxations are observed and any differences between LL-OCT and LL-BU are clearly very small.

The samples from both materials underwent cold drawing with no brittle failure observed even at −130 °C. The yield stress and strain for LL-BU are shown in Fig. 6a and b, respectively to illustrate the behaviour. The yield stress falls monotonically with temperature although the curve is not linear as for the high density material. The yield strain curve, Fig. 6b shows that it remains approximately constant up to temperatures of approximately −50 °C which corresponds to the onset of the β-relaxation. Above this temperature the yield strain, as in the HDPE, increases linearly with the temperature.

The true stress-strain curves obtained from the drawing of the slow cooled LL-BU are shown in Fig. 7 with the results being similar to those observed for the slow cooled HDPE. At temperatures below −55 °C there is a load drop as the samples form a neck and cold drawing begins but above this temperature the true stress-strain curves show no load drop. The temperature of −55 °C corresponds to the onset of the β-relaxation and interlamellar shear; therefore, in both LLDPE and HDPE the transition in the yielding process is shown to relate to the interlamellar shear process.

In Fig. 8 the nominal stress-strain curves obtained from drawing samples of slow cooled LL-BU at different strain rates show that at low strain rates only one yield point is seen whereas two are seen at high strain rates. The nominal stress-strain curves are shown because the double yield point can be more clearly resolved. Although this is similar to the results for HDPE the two yield points cannot be so clearly distinguished, probably because the necking process is less localised so that the yielding process is less pronounced. It is interesting to compare the yield strains at both yield points in LL-BU(SC) to those in HDPE(SC). The first yield point occurs at roughly the same strain of between

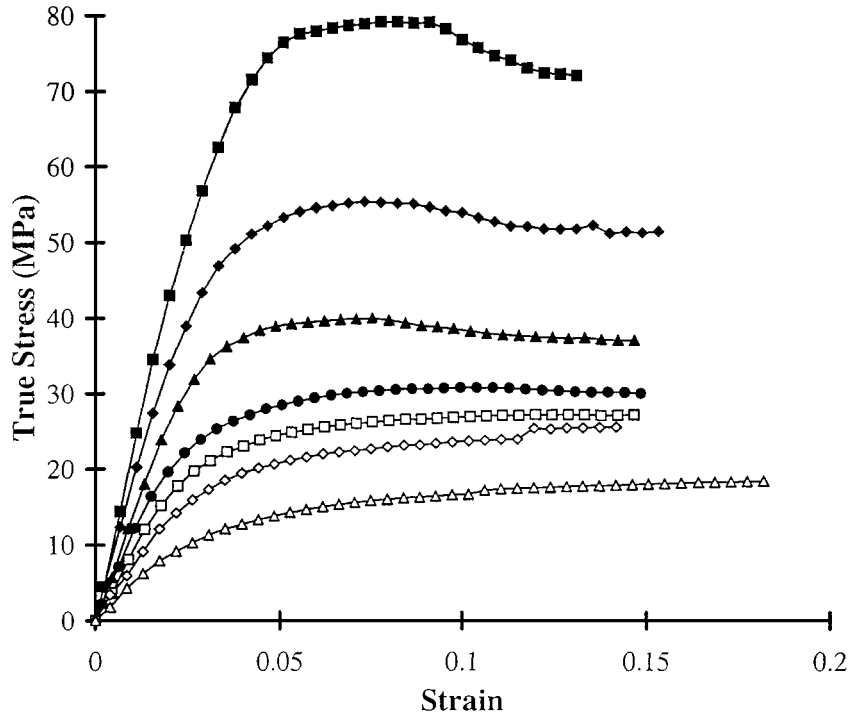

Figure 7 True stress-strain curves obtained from the uniaxial drawing of slow cooled LL-BU at an initial strain rate of $2 \times 10^{-3}\,s^{-1}$. Temperature, ■, −116 °C; ♦, −94 °C; ▲, −68 °C;●, −55 °C; □, −38 °C; ◇, −28 °C; and △, 0 °C.

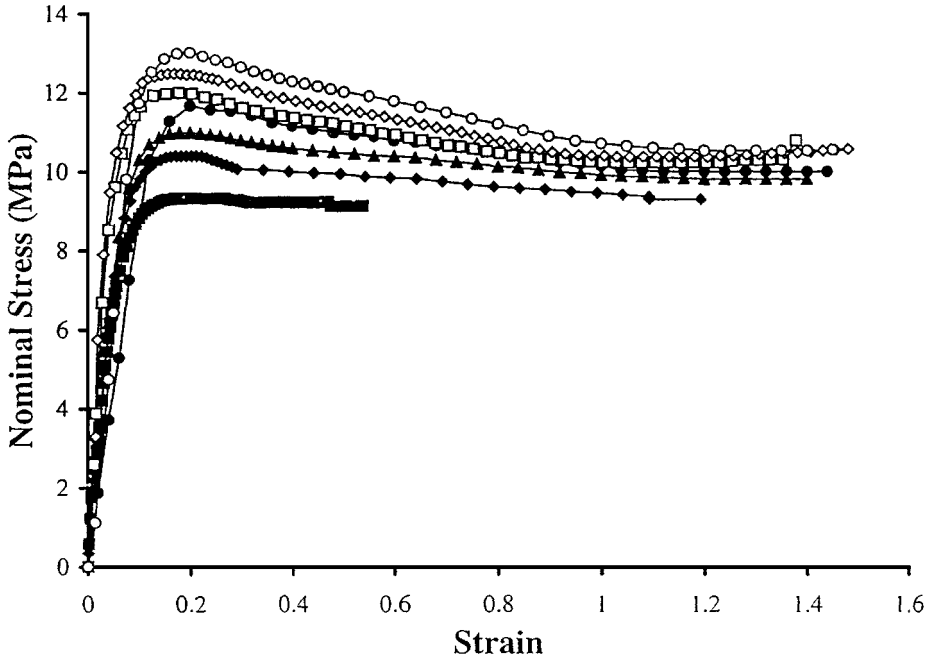

Figure 8 Nominal stress-strain curves obtained from the uniaxial drawing of slow cooled LL-BU at room temperature at a number of different strain rates. Symbols as in Fig. 4.

0.1 and 0.2 in both materials but the second yield point occurs at much lower strains in HDPE; ~0.2–0.3, compared to ~0.7 for LL-BU. The increased strain at yield can be attributed to the thinner and generally less well formed lamellae in the low density material.

4. Conclusions

It has been shown that the brittle ductile transition relates to the onset of the γ-relaxation with its short range molecular motions. The α and β-relaxations have been shown to affect the yield behaviour of both HDPE and LLDPE. The yield strain is independent of temperature before the onset of the interlamellar shear process then it increases linearly with temperature. The true stress-strain curves are also affected by the mechanical relaxations with the onset of the interlamellar shear process removing the load drop from the stress-strain curves. The two yielding processes can be seen directly in both high density and linear low density polyethylenes by drawing at high strain rates because they are then separated due to their different activation energies.

Acknowledgements

The authors would like to thank the EPSRC for funding this research project as part of the ROPA scheme and BP Chemicals Ltd. for their material assistance.

References

1. N. G. MCCRUM, B. E. READ and G. WILLIAMS, "Anelastic and Dielectric Effects in Polymeric Solids" (Dover Publications, New York, Chap. 10, 1991).
2. R. H. BOYD, *Polymer* **26** (1985) 323.
3. *Idem., ibid.* **26** (1985) 1123.
4. Z. H. STACHURSKI and I. M. WARD, *J. Polym. Sci.: A-2* **6** (1968) 1817.
5. *Idem., J. Macromol. Sci.-Phys.* **B-3** (1969) 445.
6. M. TAKAYANAGI, in Proc. Fourth Int. Cong. Rheo. (Interscience, New York, 1965) p. 161.
7. R. G. MATTHEWS, A. P. UNWIN, I. M. WARD and G. CAPACCIO, *J. Macromol. Sci-Phys.*, in press.
8. I. M. WARD, "The Mechanical Properties of Solid Polymers," 2nd ed. (John Wiley and Sons, 1983) pp. 329–432.
9. P. I. VINCENT, *Polymer* **1** (1960) 7.
10. I. HAY and A. KELLER, *Kolloid Z.* **204** (1964) 43.
11. N. W. BROOKS, R. A. DUCKETT and I. M. WARD, *Polymer*. **33** (1992) 1872.
12. *Idem., J. Rheol.* **39** (1995) 425.
13. N. W. BROOKS, A. P. UNWIN, R. A. DUCKETT and I. M. WARD, *J. Macromol. Sci-Phys.* **B34** (1995) 29.
14. A. G. GIBSON, G. R. DAVIES and I. M. WARD, *Polymer* **19** (1978) 683.
15. J. CLEMENTS, G. CAPACCIO and I. M. WARD, *J. Polym. Sci., Phys Edn* **17** (1979) 693.
16. J. D. HOFFMAN and J. J. WEEKS, *J. Chem. Phys.* **42** (1965) 4301.
17. J. D. HOFFMAN, G. WILLIAMS and E. A. PASSAGLIA, *J. Polym. Sci., A-2* **6** (1960) 1083.

Received 20 October 1998
and accepted 13 January 1999